energies

MDPI

Article

Effect of Tube Bundle Arrangement on the Performance of PCM Heat Storage Units

Maciej Fabrykiewicz and Janusz T. Cieśliński *

Faculty of Mechanical and Ocean Engineering, Gdańsk University of Technology, Narutowicza 11/12, 80233 Gdańsk, Poland
* Correspondence: jcieslin@pg.edu.pl

Abstract: The results of a comprehensive study on the charging and discharging of latent heat storage systems (LHSS) are presented. Multi-tube shell-and-tube units with variable layouts of tube bundles are examined. Two tube arrangements—in-line and staggered—are tested. A variable number of tubes and different tube positions in a bundle are investigated. Moreover, two pitch ratios are studied. Three commercially available substances are used as phase change materials (PCM). The results show that increasing the number of tubes reduces both the charging and discharging times. It is found that for a bundle of seven tubes with a pitch ratio s/d = 4.5, the in-line tube arrangement results in a shorter charging time, but the discharging time is shorter for a staggered tube arrangement.

Keywords: thermal energy storage; PCM; shell-and-tube; multi-tube; thermal performance

Citation: Fabrykiewicz, M.; Cieśliński, J.T. Effect of Tube Bundle Arrangement on the Performance of PCM Heat Storage Units. *Energies* **2022**, *15*, 9343. https://doi.org/10.3390/en15249343

Academic Editor: Artur Błaszczuk

Received: 7 November 2022
Accepted: 7 December 2022
Published: 9 December 2022

1. Introduction

Energy storage is of key importance in many areas of technology [1]. Thermal energy storage is a real challenge [2]. Thermal energy can be stored as sensible heat (SHSS), latent heat (LHSS), and thermochemically (TCES) [3]. The selection of the method of thermal energy storage depends on the source temperature. For operation temperatures above 400 °C, thermochemical reactions are used. For the same temperature range, sensible heat storage is less effective than PCM and TCES usage [4]. Due to the time mismatch between the supply of solar energy and its use, it is necessary to store thermal energy, which can then be used for heating purposes or for the preparation of hot utility water. The research carried out so far shows that the most promising way of storing thermal energy in the temperature range up to 100 °C is the use of PCMs [5]. However, the main problem in the practical application of PCMs is their low thermal conductivity, which results in low intensity of heat transfer between the heat transfer fluid (HTF) and the PCM. In practice, this means long charging and discharging times of the LHSS. The efficiency of the LHSS can be improved by using composite materials or extended heat transfer surfaces [6]. The second way is discussed in the present paper.

Hendra et al. [7] experimentally and numerically investigated the charging process of the horizontal shell- and -tube LHSSs consisting of 16 tubes in a staggered arrangement. The PCM used was a commercial product based on paraffin and animal fat. It was shown that conduction is a dominating mechanism during the initial melting period. Trp [8] numerically and experimentally studied the charging and discharging process of the vertical shell-and-tube LHSS consisting of two concentric tubes. Paraffin RT30 was used as the PCM. The results showed that the usage of water as an HTF is questionable. Only a small amount of water thermal energy was transferred to the PCM. It results from a high specific heat of the water. Agyenim et al. [9] conducted experimental studies on charging and discharging a horizontal cylindrical LHSS with a bundle of four horizontally arranged tubes. Erythritol was used as PCM. It was shown that the mean PCM temperature during LHSS charging was much higher for a bundle of tubes than for a single tube. For the

discharging process, the course of the temperature was similar beyond the initial stage of solidification. The role of free convection in multi-tube arrangements was stressed. Kibria et al. [10] numerically and experimentally studied the heat transfer in a tube-in-tube horizontal LHSS. Paraffin wax was used as the PCM. Water was used as the HTF. A numerical study revealed that the inlet temperature of HTF is a more important parameter than its mass flow rate. The tube radius, on the other hand, influences heat transfer more than the wall thickness. Esapour et al. [11] numerically investigated the influence of the number of tubes in a bundle on the paraffin RT35 melting process. The results showed that an increase in the number of tubes results in a shorter melting time, independent of the mass flow rate and the inlet temperature of the HTF. Tao and Carey [12] performed numerical simulations to study the impact of the thermophysical properties of PCMs on thermal energy and exergy storage in a tube-in-tube LHSS. The HTF was a mixture of He/Xe and salt or a salt mixture served as the PCM. The results showed that, depending on the storage time, different properties of the PCM were important. For short storage times, the main PCM properties were melting temperature and thermal conductivity, while for long storage times, the main PCM properties were density and heat of phase transition. Gasia et al. [13] experimentally investigated the charging process of an LHSS consisting of 49 smooth or finned stainless steel tubes placed in a rectangular stainless steel casing. The volume of RT58, used as the PCM, was about 0.145 m^3. It was shown that the finning of the tube surface is important during the initial stage of the charging process, when conduction is the dominant heat transfer mechanism. When more molten PCM appears, convection becomes the dominant heat transfer mechanism, and the effect of finning is negligible. Han et al. [14] numerically investigated the influence of HTF inlet configurations on the melting process of the PCM in a vertical LHSS. A eutectic mixture of KNO_3 and $NaNO_3$ served as the PCM. The calculations showed that the shortest and longest melting times were obtained for the HTF inlet at the bottom and at the top of LHSS, respectively. Kousha et al. [15] experimentally studied the impact of the inclination angle on the performance of a tube-in-tube LHSS. Paraffin RT35 was used as the PCM. The results showed that during the melting process, the heat transfer rate for a horizontal position is higher than for vertical. During the solidification process, a vertical position was more efficient. Tao et al. [16] numerically studied the influence of the PCM arrangement on the performance of a tube-in-tube LHSS. Two cases were examined. One with the PCM placed inside the tubes, and another with the PCM placed on the shell side. The volume of the PCM was the same for both cases. A salt mixture was used as the PCM. The results showed that the LHSS with the PCM inside the tubes substantially improved the thermal energy storage rate under the same working conditions and overall dimensions compared to the LHSS with the PCM on the shell side. Seddegh et al. [17] experimentally and numerically studied the influence of natural convection on the charging and discharging performance of a vertical cylindrical shell-and-tube LHSS. Paraffin RT60 was used as the PCM. A detailed analysis of the temperature distribution and melting front development was presented. Raul et al. [18] conducted an experimental investigation on the thermal performance of a vertical multitube shell-and-tube unit with a PCM on the shell side during the discharging process. Commercially available material A164 was used as the PCM. The results indicated that the intensity of the solidification process increased with an increase in the HTF mass flow rate and initial PCM temperature and with a decrease in the HTF inlet temperature. Kuta et al. [19] conducted experiments with sensible energy storage by using a shell-and-tube LHSS. CrodaTherm 53 was used as the PCM. It was shown that the heating process of water with using the LHSS was six times slower. Mehta et al. [20] experimentally and numerically studied the thermal performance of horizontal and vertical tube-in-tube units with the PCM on the shell side during the charging and discharging processes. Stearic acid was used as the PCM. The experimental results showed that the melting time of half of the PCM mass is shorter for the horizontal position than for the vertical. Kudachi et al. [21] performed an experimental and numerical study of the thermal performance of a horizontal shell-and-tube LHSS with the PCM on the shell side during the charging and

discharging process. Commercially available organic mixture OM65 was used as the PCM. It was established that the charging process is twice as long as the discharging stage. The PCM temperature resulting from the numerical calculations was 5 to 10 K higher than the measured temperature, which was attributed to the heat losses which were not included in the calculations. Mahdi et al. [22] numerically investigated the influence of 3 tube bundle arrangements on the charging efficacy of the LHSS. The shortest melting time was observed for the tubes which were very close to the bottom of the LHSS. Shaikh et al. [23] numerically analyzed the effect of the number of tubes on the PCM melting time in the system when the LHSS shell was also heated. The melting time of the PCM in the system with a heated shell was about five times shorter compared to the double-tube system. Mahdavi et al. [24] numerically examined the performance of the LHSS consisting of four tubes interconnected by thin longitudinal fins. Two of the tubes were supplied with hot fluid and two with cold fluid. Thus, the LHSS was simultaneously charged and discharged. The amount of stored energy was the highest for the case when the hot HTF tubes were in the lower half of the LHSS. Qaiser et al. [25] numerically and experimentally studied the effect of Y-finning and the cross-section of the shell on the PCM melting process. It was established that the melting time decreased as the number of Y-finned tubes increased. The triangular shell was shown to be more advantageous than a cylindrical shell. Song et al. [26] showed numerically that the use of tree-shaped fins shortens the melting time of PCM by a factor of five. Vikas et al. [27] numerically studied the charging process of an LHSS consisting of a bundle of five tubes. A total of 10 cases of tube positioning have been proposed. The shortest melting time was obtained for the system in which the tube in the upper half was shifted towards the central tube and the tube in the lower half was moved downwards from the central tube. In [28], Vikas et al. numerically studied the effect of in-line and staggered tube arrangements on the melting time for a bundle of four tubes. The shortest melting time was obtained for the staggered layout with finned tubes. Qaiser et al. [29] numerically investigated the influence of the external cross-section of the HTF tubes on the melting process. In total, eight combinations of a system of three tubes with four cross-sections were analyzed. It was established that the tube bundle with triangular tubes outperformed the other cases. Zaglanmis et al. [30] numerically studied the melting process of four different PCMs placed in the shell side of a horizontal multi-tube LHSS. It was observed that the melting rate and stored energy increased with an HTF inlet temperature increase. Regardless of the tested PCMs, it was established, that the melting time decreased with an HTF inlet temperature increase.

In this paper, the results of experimental investigations on the charging and discharging of horizontal multi-tube LHSSs are presented. Three commercial products, LTP56, RT54HC, and P1808 from the group of aliphatic hydrocarbons were used as PCMs. The tests included two tube arrangements, namely, in-line and staggered, a variable number of tubes in a bundle from four to seven, two pitch ratios (4.5 and 5.0), and different tube positions in a bundle with the same number of tubes. Although there are several papers in the published literature on the influence of the tube arrangement and number of tubes on LHSS performance, to the best of the authors' knowledge, there is not a single paper that addresses the influence of the pitch ratio.

2. Materials and Methods

The experimental rig consists of four basic sections: LHSS, cold water loop, hot water loop, and PC-aided data acquisition system. The view of the experimental stand is shown in Figure 1.

2.1. Tested LHSS

The cylindrical LHSS was composed of acrylic glass. The outside diameter of the shell was 80 mm, and the length was 400 mm. The thickness of the wall was 5 mm. The tubes from which the bundle was produced were composed of stainless steel 1.4301. The outside

diameter of the tube was 6 mm, and the wall thickness was 1 mm. A view of the tested LHSS is shown in Figure 2.

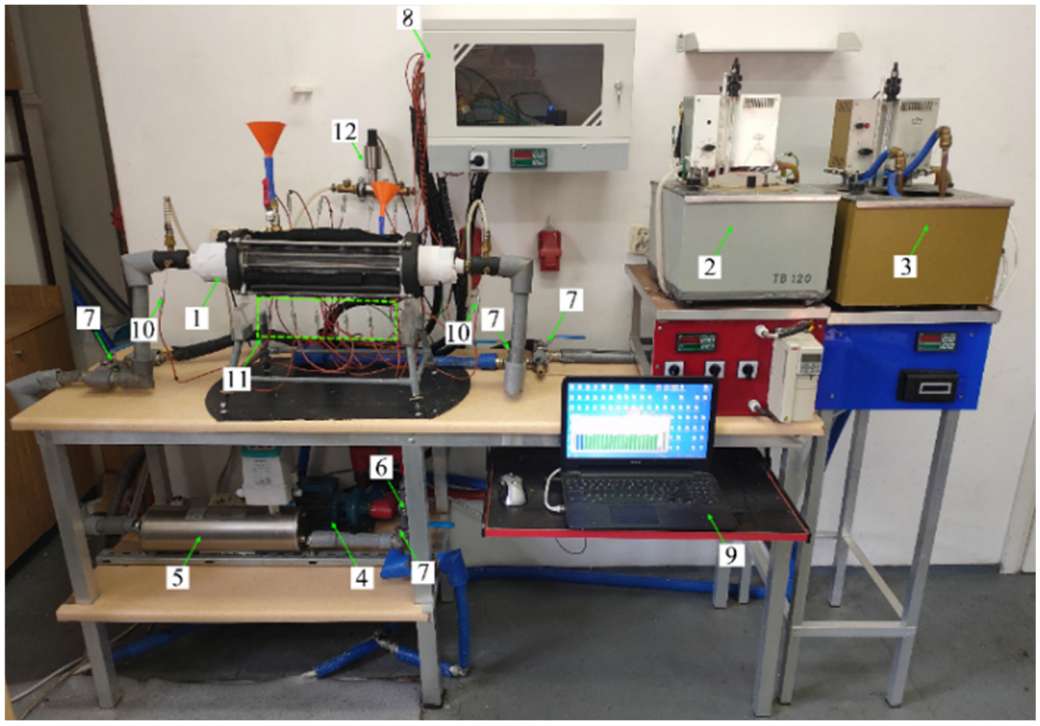

Figure 1. View of the experimental stand: 1—LHSS, 2—hot water thermostat, 3—cold water thermostat, 4—pump, 5—ultrasonic flow meter, 6—needle valve, 7—three-way valve, 8– multiplexer, 9—PC, 10–11– resistance thermometer, 12—pressure difference transducer.

Figure 2. View of the tested LHSS.

The temperature distribution in the PCM was determined by using eighteen Pt100 resistance thermometers—T1-T18 in Figure 3. The shield diameter of the resistance thermometers was 1.5 mm. The PCM temperature distribution was measured in 6 sections and in each section in 3 radii, as shown in Figure 3.

The tested tube arrangements are shown in Table 1. The tests were carried out for in-line and staggered tube arrangements. The number of tubes in a bundle was changed from 4 to 7. Two pitch ratios, namely, $s/d = 4.5$ and $s/d = 5.0$, were examined. Moreover, for the same number of tubes, various tubes placements in the shell were tested.

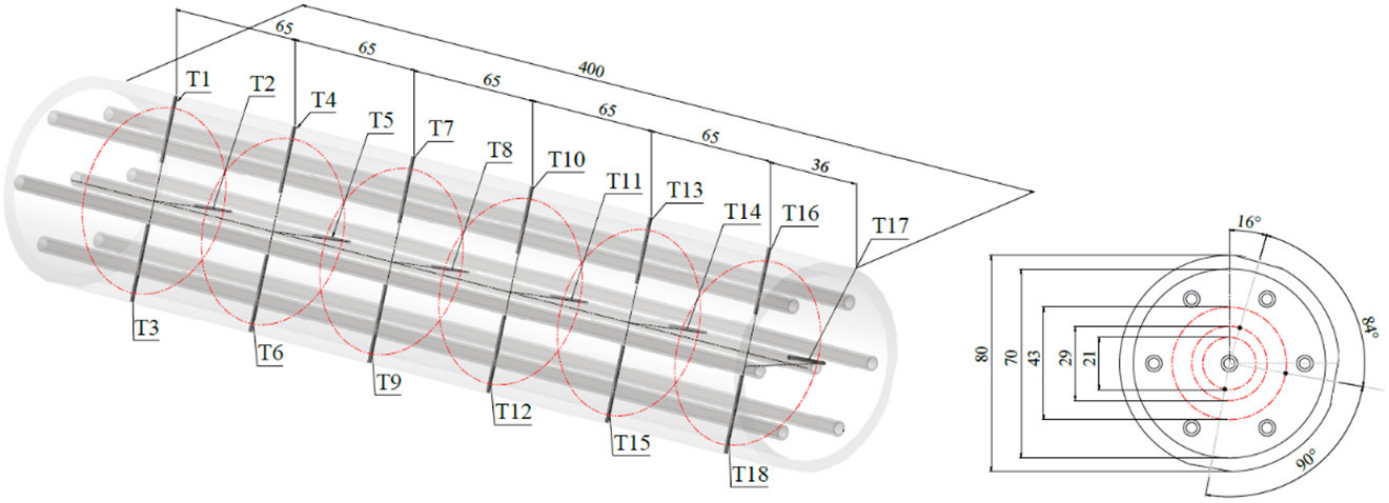

Figure 3. Distribution of PCM temperature measurement points.

Table 1. Tested tube arrangements.

Tube Arrangement	Number of Tubes	Tube Position/Pitch Ratio		Filling the Shell [%]
		s/d = 5.0	s/d = 4.5	
In-line	7			5.1
	6			4.4
				
	5			3.7
	4			2.9
Staggered	7			5.1
	6			4.4
	5			3.7

2.2. Materials

Three commercially available substances were tested. The choice of PCMs was based on three reasons. First, the range of the melting temperature corresponds to the systems with solar collectors and underfloor heating. Second, the selected PCMs are organic substances, two of which belong to the group of fatty acids and one to paraffin. Third, the high availability and reasonable price of the used PCMs, which was important due to

the large number of tests performed. The specifications of the tested PCMs are shown in Table 2.

Table 2. Materials characteristics.

Product	Substance	Chemical Formula	Fraction	
LTP56 Polwax S.A. [31]	Paraffin	$C_{19}H_{38}$ to $C_{32}H_{65}$	100%	
RT54HC Rubitherm Technologies [32]	Fatty acid	$C_{14}H_{28}O_2$	97%	
P1808 Konimpex Chemicals [33]	Fatty acid	$C_{16}H_{32}O_2$ Palmitic acid	58%	96%
		$C_{17}H_{35}O_2$ Stearic acid	38%	

The results of the DSC analysis are presented in Table 3.

Table 3. DSC characteristics of the tested materials.

Parameter	LTP56	RT54HC	P1808
t_m^h [°C]	33.9–63.2	46.7–66.1	48.3–65.9
t_m^c [°C]	40.1–54.9	37.9–52.8	38.1–53.5
c_{p_s} [J/(gK)]	2.19	2.46	1.96
c_{p_l} [J/(gK)]	2.21	2.59	2.25
r_m^h [J/g]	159.4	220.6	178.5

2.3. Experimental Procedure

All measurements started with the discharging process. Using a cold water loop with the proper settings of three-way valves (Figure 1), the temperature of the LHSS was set at 20 °C ± 0.5 K. This process continued for about 10 min. At 80 °C, the PCM was then poured into the shell. The LHSS pouring time was about 20 s. After this time, the PCM temperature distribution of the PCM was recorded. The end of the discharging process was considered to be the state in which each resistance thermometer indicated a temperature of 22 °C ± 0.5 K. The charging process started with heating up the assembly without the LHSS to the temperature of 80 °C ± 0.5 K. For this purpose, a hot water loop was used with the proper adjustment of three-way valves (Figure 1). This process continued for about 10 min. After this time, the recording of the PCM temperature distribution started. The charging process was finished when the mean PCM temperature differed by ±0.5 K for 15 min.

2.4. Measurement Uncertainty

The average PCM temperature was calculated as the arithmetic mean of the indications of 18 resistance thermometers placed on the shell side—Figure 3.

$$t = \frac{\sum_1^{18} t_i}{18} \tag{1}$$

The uncertainty of the average temperature was estimated by the mean-square method as

$$\Delta t = \sqrt{\left(\frac{\partial t}{\partial t_1}\Delta t_1\right)^2 + \left(\frac{\partial t}{\partial t_2}\Delta t_2\right)^2 + \ldots + \left(\frac{\partial t}{\partial t_{18}}\Delta t_{18}\right)^2} \tag{2}$$

where the absolute measurement error of the temperature by using a Pt100 resistance thermometer is $\Delta t_i = 0.5$ K. Therefore, the maximum overall experimental limit of error for the average temperature extended from ±0.14% for the maximum temperature up to ±0.58% for the minimum temperature.

3. Results and Discussion

In order to validate the measurement procedure, two day-by-day charging and discharging cycles were conducted. In Figure 4a,b the results for LTP56 and P1808 are presented. Very good repeatability of the results was obtained for both PCMs and tube arrangements. The temperature distributions for the two runs corresponding to the charging and discharging processes practically coincide.

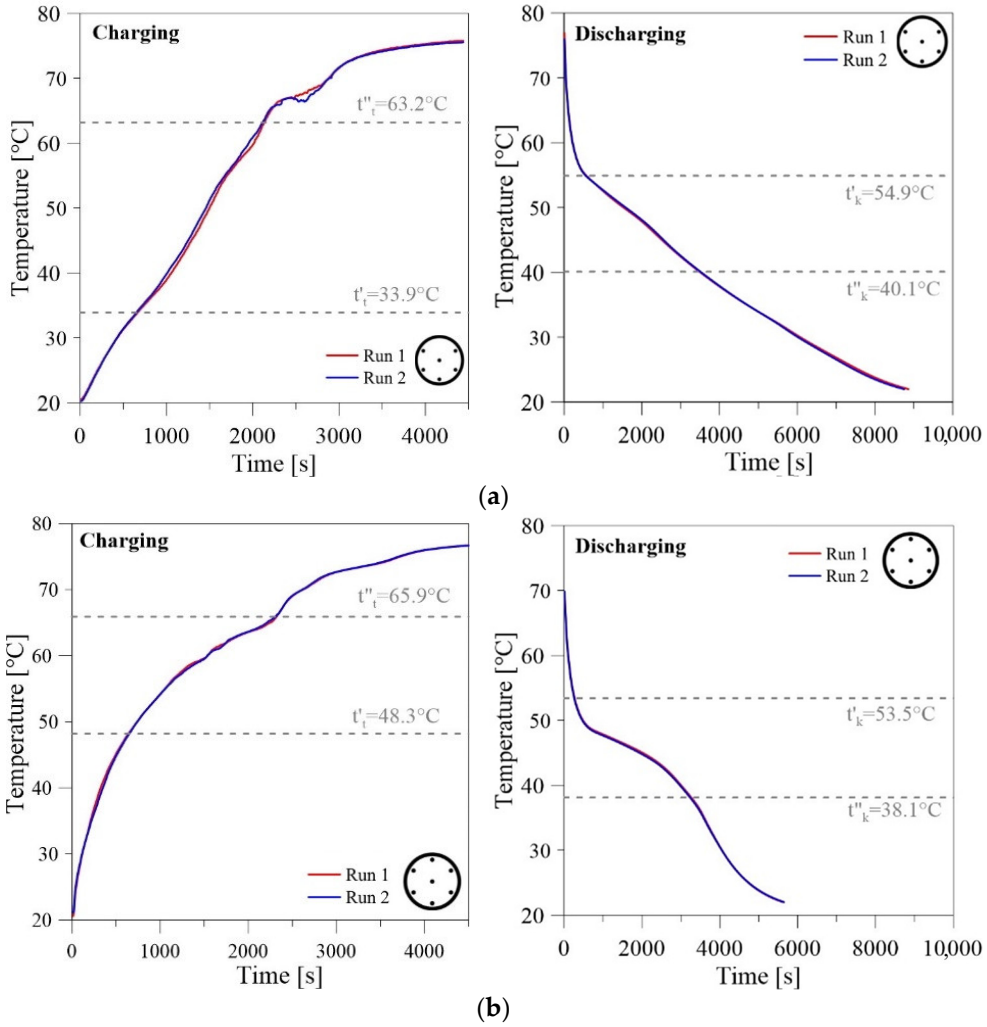

Figure 4. Repeatability of PCM temperature measurements: (**a**) LTP56; (**b**) P1808.

3.1. Effect of the Number of Tubes in A Bundle

Figure 5 shows the average PCM P1808 temperature course during the charging and discharging process for an in-line tube bundle with the number of tubes varying from four to seven. Figure 5a,b clearly shows that an increase in the number of tubes, thus increasing the heat transfer surface, shortens the time for both the charging and discharging of the LHSS. The shortest melting and solidification time of the LHSS was obtained for a bundle of seven tubes—red lines in Figure 5a,b. However, it should be noted that two cases with six tubes were tested: one in which all tubes were placed circumferentially around the shell (green), and the other in which the top tube was placed centrally (blue). As can be seen in Figure 5a, the time to reach the final melting temperature for the bundle of six tubes placed circumferentially around the shell (green line) is slightly shorter than that for the bundle of four tubes (black line) but with the tube placed centrally. On the other hand, increasing the number of tubes from six (blue line) to seven (red line) in bundles with the tube placed centrally resulted in only a slight shortening of the PCM melting time.

The progress of the melting process is therefore controlled by the centrally located tube, which determines the development of free convection in the bundle of tubes. Similar to the melting process, the central tube is critical to the solidification process. As can be seen in Figure 5b, the time to reach the final solidification temperature for a bundle of six tubes placed circumferentially around the shell (green) is even longer than for a bundle of four tubes but with the tube placed centrally (black line). This is understandable because the progress of the solidification process is determined by heat conduction. Due to the lack of a central tube, the thickness of the solidified PCM is almost equal to the radius of the shell, and, therefore, the time it takes for the solidification front to reach the center of the LHSS is the longest. Similar to the melting process, increasing the number of tubes from six (blue line) to seven (red line) in bundles with the tube placed centrally resulted in only a slight shortening of the PCM solidification time—Figure 5b.

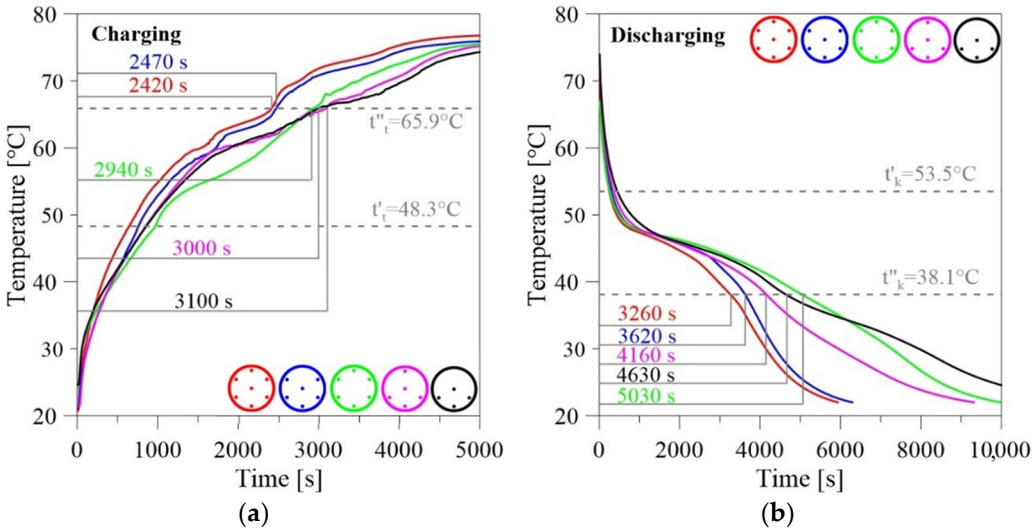

Figure 5. Effect of the number of tubes for P1808: (**a**) charging; (**b**) discharging.

Figure 6 shows the average PCM LTP56 temperature course during the charging and discharging process for the staggered tube bundle with the number of tubes varying from five to seven. As seen in Figure 6, the average temperature during the entire charging process was the highest and the lowest for a bundle consisting of seven tubes (red lines in Figure 6a,b). As with the in-line arrangement, the central tube plays a key role in the development and progress of the melting and solidification process.

3.2. Effect of the Tube Arrangement

Figure 7 shows the average PCM temperature distribution during the charging and discharging process of LTP56 for the in-line and staggered tube arrangements for the bundle of seven tubes and the same pitch ratio of s/d = 4.5.

As shown in Figure 7a, in the initial period of LHSS charging, the rate of temperature increases in the solidified PCM is slightly higher for the staggered layout than for the in-line arrangement. During this period, the solidified PCM at 20 °C is in contact with the surface of the tubes in which HTF flows at a temperature of 80 °C. The dominant heat transfer mechanism is conduction. After about 300 s, the PCM reaches its initial melting temperature, and the amount of molten PCM begins to build up around the tubes. After about 1000 s, the slope of the temperature distribution curve for the in-line layout is steeper than for the staggered layout. This temperature distribution results from the increasing role of free convection, which becomes the dominant mechanism of heat transfer. The reason why the in-line layout is preferable to the staggered layout is that in the in-line arrangement, the tubes in the upper rows are placed in the convective wakes formed on the tubes below. Therefore, the time to reach the final melting temperature for the in-line

layout (1650 s) is clearly shorter than for the staggered layout (2290 s). The research shows that the staggered tube layout results in a shorter discharging time for the tested PCMs. As shown in Figure 7b, in the initial period of PCM solidification, the temperature drop is very rapid and results from the contact of molten PCM at 80 °C with tube surfaces in which flows HTF at 20 °C. During this period, the dominant heat transfer mechanism is free convection, but a layer of solidified PCM forms around the tubes, which increases in thickness over time. As shown in Figure 7b, after about 500 s, the thickness of this layer is so large that the rate of temperature drop clearly decreases, which is the same for both tube layouts. This indicates that the dominant heat transfer mechanism is conduction in the solidified PCM layer, and the arrangement of the tubes is no longer relevant.

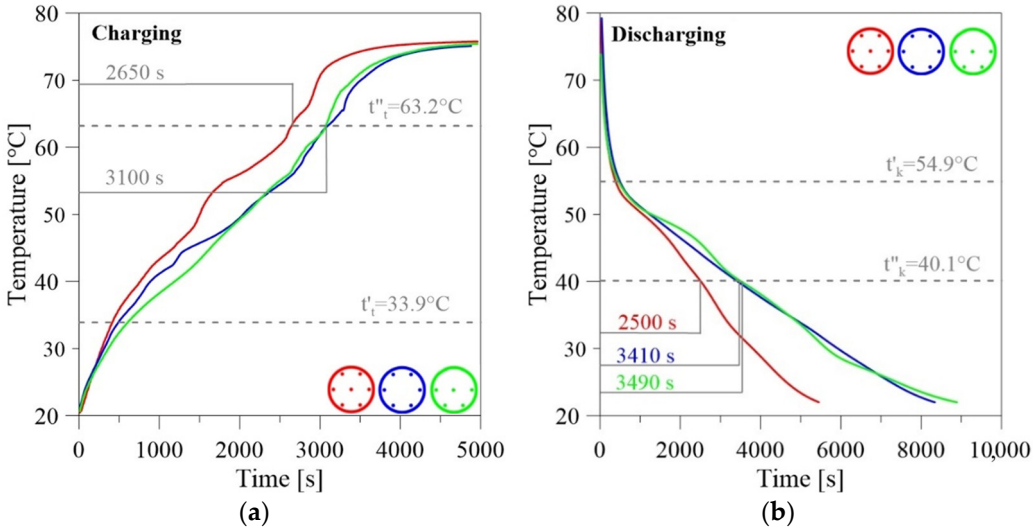

Figure 6. Effect of the number of tubes for LTP56: (**a**) charging; (**b**) discharging.

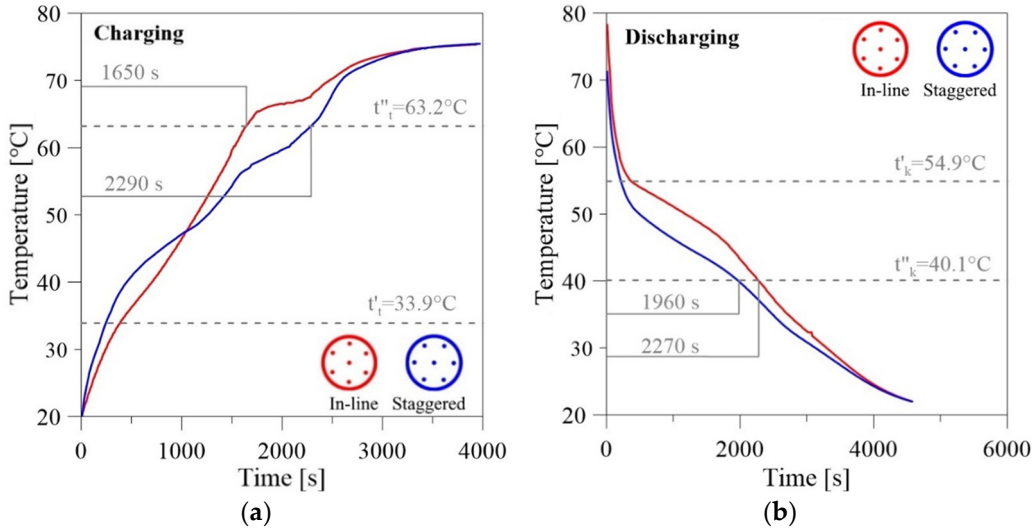

Figure 7. Effect of the tube arrangement for LTP56: (**a**) charging; (**b**) discharging.

3.3. Effect of the Pitch Ratio

Figure 8 shows the temperature course of RT54HC for the staggered tube arrangement and two pitch ratios, namely, s/d = 4.5 and s/d = 5.0.

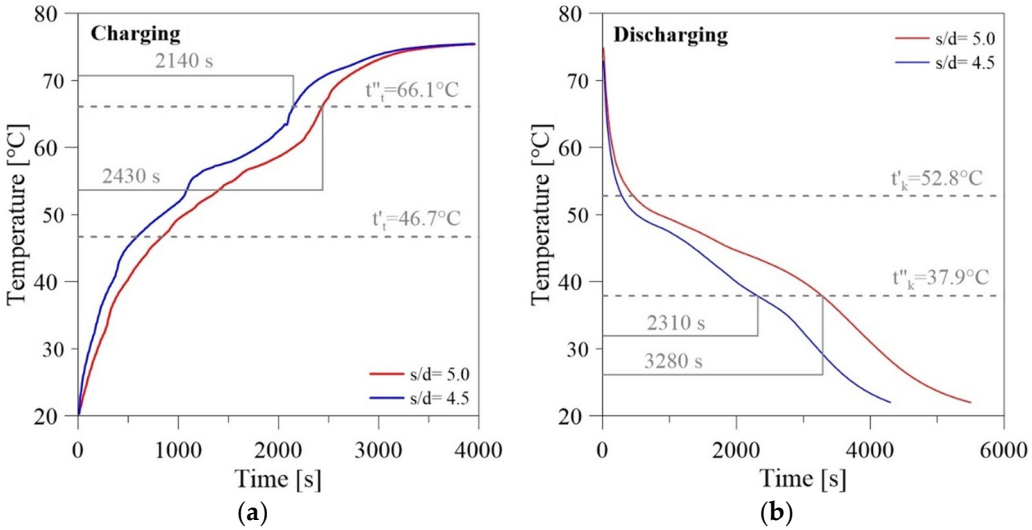

Figure 8. Effect of the pitch ratio for RT54HC: (**a**) charging, (**b**) discharging.

The pitch ratio is the ratio of the distance between adjacent tubes to the outside diameter of the tube [34]. Hence, for a given diameter, a smaller pitch ratio means a smaller distance between adjacent tubes. As shown in Figure 8a,b, the time to reach the final melting and solidification temperature is shorter for the smaller tested pitch ratio (blue lines). The shorter melting time for a tube bundle with a smaller pitch ratio results from more intense heat transfer caused by free convection. It is obvious that the influence of convection currents is more intense as the distance between the tubes is smaller. On the other hand, in the case of solidification, a smaller distance between the tubes means a smaller thickness of the solidified PCM layer, and, therefore, a lower heat conduction resistance, and hence a shorter solidification time.

4. Conclusions

This paper presents the experimental results of a shell-and-tube horizontal LHSS. In particular, the influence of the tube bundle geometry on the charging and discharging times of the LHSS was investigated. A total of 16 different cases were examined.

The main conclusions are as follows:

- Regardless of the tube layout, the shortest charging/discharging time was obtained for the bundle with the largest tested number of tubes, namely, seven.
- Studies have shown that in addition to increasing the number of tubes, and thus the heat transfer surface, the arrangement of the tubes is no less important. The centrally located tube is extremely important, as it affects the progress of both the melting and solidification processes.
- The staggered tube arrangement outperformed the in-line tube layout for the discharging process. For the charging process, the opposite is true.
- Out of the two pitch ratios tested, namely, s/d = 4.5 and s/d = 5, the smaller pitch ratio results in shorter charging and discharging times.
- The conclusions presented are for a small LHSS with only a few tubes. Further investigations, including numerical ones, are necessary for the much larger LHSSs with large numbers of tubes.

Author Contributions: Conceptualization, J.T.C. and M.F.; methodology, M.F. and J.T.C.; software, M.F.; validation, J.T.C. and M.F.; formal analysis, J.T.C. and M.F.; investigation, M.F.; data curation, M.F.; writing—original draft preparation, J.T.C.; writing—review and editing, J.T.C. and M.F.; funding acquisition, J.T.C. All authors have read and agreed to the published version of the manuscript.

Funding: This research received no external funding.

Conflicts of Interest: The authors declare no conflict of interest.

Nomenclature

c_p	Specific heat at constant pressure	[J/(kgK)]
d	Tube diameter	(m)
r	Heat of phase transition	[J/kg]
s	Pitch	(m)
t	Temperature	(°C)

Subscripts

k	Solidification
l	Liquid
m	Phase change
s	Solid
t	Melting

Superscripts

c	Cooling
h	Heating
′	Beginning
″	End

Abbreviations

DSC	Digital Scanning Calorimetry
HTF	Heat Transfer Fluid
LHSS	Latent Heat Storage System
PCM	Phase Change Material
SHSS	Sensible Heat Storage System
TCES	Thermochemical Energy Storage

References

1. Letcher, T.M. *Storing Energy with Special Reference to Renewable Energy Sources*; Elsevier: Amsterdam, The Netherlands, 2016.
2. Domański, R. *Conversion and Accumulation of Energy. Selected Problems*; Biblioteka Naukowa Instytutu Lotnictwa nr 54. Sieć Badawcza Łukasiewicz—IL: Warsaw, Poland, 2020. (In Polish)
3. Cabeza, L.F. (Ed.) *Advances in Thermal Energy Storage Systems: Methods and Applications*; Woodhead Publishing Series in Energy; Elsevier: Amsterdam, The Netherlands, 2015.
4. Faninger, G. Thermal Energy Storage. 2005. Available online: http://www.celsius.co.kr/phase_change_materials/download/energy/Thermal_Energy_Storage.pdf (accessed on 21 January 2016).
5. Fredi, G.; Dorigato, A.; Fambri, L.; Pegoretti, A. Evaluating the multifunctional performance of structural composites for thermal energy storage. *Polymers* **2021**, *13*, 3108. [CrossRef] [PubMed]
6. Khan, Z.; Khan, Z.; Ghafoor, A. A review of performance enhancement of PCM based latent heat storage system within the context of materials, thermal stability and compatibility. *Energy Convers. Manag.* **2016**, *115*, 132–158.
7. Hendra, R.; Hamdani; Mahlia, T.M.I.; Masjuki, H.H. Thermal and melting heat transfer characteristics in a latent heat storage system using Mikro. *Appl. Therm. Eng.* **2005**, *25*, 1503–1515. [CrossRef]
8. Trp, A. An experimental and numerical investigation of heat transfer during technical grade paraffin melting and solidification in a shell-and-tube latent thermal energy storage unit. *Sol. Energy* **2005**, *79*, 648–660. [CrossRef]
9. Agyenim, F.; Eames, P.; Smyth, M. Heat transfer enhancement in medium temperature thermal energy storage system using a multitube heat transfer array. *Renew. Energy* **2010**, *35*, 198–207. [CrossRef]
10. Kibria, M.A.; Anisur, M.R.; Mahfuz, M.H.; Saidur, R.; Metselaar, I.H.S.C. Numerical and experimental investigation of heat transfer in a shell and tube thermal energy storage system. *Int. Commun. Heat Mass Transf.* **2014**, *53*, 71–78.
11. Esapour, M.; Hosseini, M.J.; Ranjbar, A.A.; Pahamli, Y.; Bahrampoury, R. Phase change in multi-tube heat exchangers. *Renew. Energy* **2016**, *85*, 1017–1025. [CrossRef]
12. Tao, Y.B.; Carey, V.P. Effects of PCM thermophysical properties on thermal storage performance of a shell-and-tube latent heat storage unit. *Appl. Energy* **2016**, *179*, 203–210.

13. Gasia, J.; Diriken, J.; Bourke, M.; Van Bael, J.; Cabeza, L.F. Comparative study of the thermal performance of four different shell-and-tube heat exchangers used as latent heat thermal energy storage systems. *Renew. Energy* **2017**, *114*, 934–944. [CrossRef]
14. Han, G.S.; Ding, H.S.; Huang, Y.; Tong, L.G.; Ding, Y.L. A comparative study on the performances of different shell-and-tube type latent heat thermal energy storage units including the effects of natural convection. *Int. Commun. Heat Mass Transf.* **2017**, *88*, 228–235.
15. Kousha, N.; Hosseini, M.J.; Aligoodarz, M.R.; Pakrouh, R.; Bahrampoury, R. Effect of inclination angle on the performance of a shell and tube heat storage unit—An experimental study. *Appl. Therm. Eng.* **2017**, *112*, 1497–1509. [CrossRef]
16. Tao, Y.B.; Liu, Y.K.; He, Y.L. Effects of PCM arrangements and natural convection on charging and discharging performance of the shell-and-tube LHS unit. *Int. J. Heat Mass Transf.* **2017**, *115*, 99–107. [CrossRef]
17. Seddegh, S.; Joybari, M.M.; Wang, X.; Haghighat, F. Experimental and numerical characterization of natural convection in a vertical shell-and-tube latent thermal energy storage system. *Sustain. Cities Soc.* **2017**, *35*, 13–24. [CrossRef]
18. Raul, A.K.; Bhavsar, P.; Saha, S.K. Experimental study on discharging performance of vertical multitube shell and latent thermal energy storage. *J. Energy Storage* **2018**, *20*, 279–288.
19. Kuta, M.; Matuszewska, D.; Wójcik, T.M. Design of PCM based heat exchangers constructions for thermal energy storage tanks—Examples and case study for selected design. *E3S Web Conf.* **2018**, *70*, 01010. [CrossRef]
20. Mehta, D.S.; Solanki, K.; Rathod, M.K.; Banerjee, J. Thermal performance of shell and tube latent heat storage unit: Comparative assessment of horizontal and vertical orientation. *J. Energy Storage* **2019**, *23*, 344–362.
21. Kudachi, B.; Varkute, N.; Mashilkar, B.; Guthulla, S.; Jayaprakash, P.; Aaron, A.; Joy, S. Experimental and computational study of phase change material based shell and tube heat exchanger for energy storage. *Mater. Today Proc.* **2021**, *46*, 10015–10021.
22. Mahdi, M.S.; Mahood, H.B.; Alammar, A.A.; Khadom, A.A. Numerical investigation of PCM melting using different tube configurations in a shell and tube latent heat thermal storage unit. *Therm. Sci. Eng. Prog.* **2021**, *25*, 101030. [CrossRef]
23. Shaikh, M.; Uzair, M.; Allauddin, U. Effect of geometric configurations on charging time of latent-heat storage for solar applications. *Renew. Energy* **2021**, *179*, 262–271. [CrossRef]
24. Mahdavi, A.; Moghaddam, M.A.E.; Mahmoudi, A. Simultaneous charging and discharging of multi-tube heat storage systems using copper fins and Cu nanoparticles. *Case Stud. Therm. Eng.* **2021**, *27*, 101343.
25. Qaiser, R.; Khan, M.M.; Khan, L.A.; Irfan, M. Melting performance enhancement of PCM based thermal energy storage system using multiple tubes and modified shell designs. *J. Energy Storage* **2021**, *33*, 102161. [CrossRef]
26. Qaiser, R.; Khan, M.M.; Ahmed, H.F.; Malik, F.K.; Irfan, M.; Ahad, I.U. Performance enhancement of latent energy storage system using effective designs of tubes and shell. *Energy Rep.* **2022**, *8*, 3856–3872. [CrossRef]
27. Song, L.; Wu, S.; Yu, C.; Gao, W. Thermal performance analysis and enhancement of the multi-tube latent heat storage (MTLHS) unit. *J. Energy Storage* **2022**, *46*, 103812. [CrossRef]
28. Yadav, A.; Samir, S.; Arıcı, M. A comprehensive study on melting enhancement by changing tube arrangement in a multi-tube latent heat thermal energy storage system. *J. Energy Storage* **2022**, *55 Pt B*, 105517.
29. Yadav, A.; Samir, S. Melting dynamics analysis of a multi-tube latent heat thermal energy storage system: Numerical study. *Appl. Therm. Eng.* **2022**, *214*, 118803.
30. Zaglanmis, E.; Demircan, T.; Gemicioglu, B. Analysis of melting behaviours of phase change materials used in heat energy storage systems. *Heat Transf. Res.* **2022**, *53*, 31–46.
31. Offer. Available online: www.polwax.pl/oferta/dla-przemyslu-swiecowego (accessed on 25 August 2018).
32. Products. Available online: www.rubitherm.eu/en/index.php/productcategory/organische-pcm-rt (accessed on 9 October 2020).
33. Chemicals. Available online: www.konimpexchemicals.com.pl/kategoria/oleochemikalia (accessed on 16 February 2017).
34. Gupta, J.P. *Fundamentals of Heat Exchanger and Pressure Vessel Technology*; Hemisphere: Washington, DC, USA, 1986.